Nanostructured Hybrid Materials Formed by Sequestration of Pyridine Molecules in the Tunnels of Sepiolite

Wenxing Kuang,[†] Glenn A. Facey,[†] Christian Detellier,*[,†] Blanca Casal,[‡] José M. Serratosa,[‡] and Eduardo Ruiz-Hitzky*[,‡]

Center for Catalysis Research and Innovation and Department of Chemistry, University of Ottawa, Ottawa, Ontario, Canada K1N6N5, and Instituto de Ciencia de Materiales de Madrid, CSIC, E-28049 Cantoblanco, Madrid, Spain

Received September 16, 2003. Revised Manuscript Received October 24, 2003

The process of incorporation of pyridine in the nanostructured tunnels of sepiolite was studied in detail, using various complementary characterization techniques, microporosimetry, thermal gravimetric analysis, FTIR, and multinuclear solid-state NMR. It is demonstrated that a remarkable nanohybrid material, SEP−PYR, is formed through the direct coordination of pyridine to the edge Mg(II) sites of the tunnels. This material is formed at temperatures above 140 °C when the sepiolite tunnels are dehydrated and the pyridine molecules are trapped in the tunnels. In a first step toward the formation of SEP−PYR, the pyridine molecules were incorporated at room temperature in the tunnels, by exposing sepiolite to pyridine vapors. The incorporated pyridine molecules are H-bound to the structural water molecules coordinated to the edge Mg(II) cations. In a second step, upon heating to 140 °C, approximately 50% of the pyridine is lost, together with most of the structural water coordinated to Mg(II). This event is accompanied by direct coordination of the remaining pyridine molecules in the tunnels to the edge Mg(II) ions of the octahedral sheets, resulting in a material with a structure similar to the parent sepiolite, but with pyridine molecules coordinated to the Mg(II) edge cations. This material is stable up to 450 °C. At this temperature, the coordinated pyridine molecules escape from the tunnels, resulting in a collapsed sepiolite structure.

Introduction

Among the naturally occurring alumino and/or magnesio silicates belonging to the clay minerals group, two minerals, sepiolite and palygorskite, have a very special place due to their particular crystal structure, microfibrous morphology,[1] and their useful ability to adsorb molecular, ionic, and polymeric species.[2−4] Although one of their most striking applications was their use by the Mayas to prepare a blue pigment (Maya Blue),[4] both sepiolite and palygorskite are receiving a great deal of attention nowadays because they are used in many different applications.[5] Recently, it was shown that sepiolite could be used to make membranes suitable for ultrafiltration,[6] or, with zeolites, for gas separation.[7] The potential to use sepiolite and its derivatives for advanced applications such as active and specific adsorb-

* Authors to whom correspondence should be addressed. E-mail: dete@science.uottawa.ca (C. Detellier); eduardo@icmm.csic.es (E. Ruiz-Hitzky).

[†] University of Ottawa.

[‡] CSIC.

(1) (a) Serratosa, J. M. In *Proceedings International Clay Conference*, 1978; Elsevier Sci. Publ.: Amsterdam, 1979; pp 99−109. (b) Jones, B. F.; Galan, E. In R*eviews in Mineralogy*; Bailey, S. W., Ed.; Mineralogical Society of America: Washington D.C., 1988; Vol. 19 (Hydrous Phyllosilicates); Chapter 16 (Sepiolite and palygorskite), pp 631−674.

(2) (a) Barrer, R. M.; Mackenzie, N. *J. Phys. Chem.* **1954**, *58*, 560−568. (b) Barrer, R. M.; Mackenzie, N.; MacLeod, D. M. *J. Phys. Chem.* **1954**, *58*, 568−575. (c) Serna, C.; Fernandez-Alvarez, T. *Anal. Quim.* **1974**, *70*, 760−764. (d) Serna, C. J.; Vanscoyoc, G. E. In *Proceedings International Clay Conference* 1978; Elsevier Sci. Publ.: Amsterdam, 1979; pp 197−206. (e) Inagaki, S.; Fukushima, Y.; Doi, H.; Kamigaito, O. *Clay Miner.* **1990**, *25*, 99−105. (f) Rytwo, G.; Nir, S.; Margulies, L.; Casal, B.; Merino, J.; Ruiz-Hitzky, E.; Serratosa, J. M. *Clays Clay Miner.* **1998**, *46*, 340−348. (g) Weir, M. R.; Facey, G. A.; Detellier, C. *Stud. Surf. Sci. Catal.* **2000**, *129*, 551−558. (h) Rytwo, G.; Tropp, D.; Serban, C. *Appl. Clay Sci.* **2002**, *20*, 273−282. (i) Shariatmadari, H.; Mermut, A. R.; Benke, M. B. *Clays Clay Miner.* **1999**, *47*, 44−53. (j) Akyüz, S.; Akyüz, T. *J. Mol. Struct.* **2003**, *205*−*210*, 651−653. (k) Balci, S. *Clay Miner.* **1999**, *34*, 647−655. (l) d'Espinose de la Caillerie, J.-B.; Gruver, V.; Fripiat, J. J. *J. Catal.* **1995**, *151*, 420−430.

(3) Ruiz-Hitzky, E. *J. Mater. Chem.* **2001**, *11*, 86−91.

(4) (a) Gettens, R. J. *Am. Antiquity* **1962**, *27*, 557−564. (b) Shepard, A. *Am. Antiquity* **1962**, *27*, 565−566. (c) Van Olphen, H. *Science* **1966**, *154*, 645−646. (d) Kleber, R.; Masschelein-Kleiner, L.; Thissen, J. *Stud. Conserv.* **1967**, *12*, 41−56. (e) Yacamán, M. J.; Rendon, L.; Arenas, J.; Puche, M. C. S. *Science* **1996**, *273*, 223−225. (f) Polette, L. A.; Meitzner, G.; Yacamán, M. J.; Chianelli, R. R. *Microchem. J.* **2002**, *71*, 167−174. (g) Hubbard, B.; Kuang, W.; Moser, A.; Facey, G. A.; Detellier, C. *Clays Clay Min.* **2003**, *51*, 318−326. (h) Fois, E.; Gamba, A.; Tilocca, A. *Microporous Mesoporous Mater.* **2003**, *57*, 263−272. (i) Sánchez del Rio, M.; Reyes-Valerio, C.; Somogyi, A.; Martinetto, P.; Dooryhée, S.; Suárez Barrios, M.; Alianelli, L.; Felici, R. *Abstracts of the 10th Conference of the European Clay Groups Association*, EuroClay 2003, Modena, Italy, 2003; pp 247−248.

(5) (a) Chambers, G. P. C. *Silic. Ind.* **1959**, *24*, 181. (b) Alvarez, A. In *Palygorskite−Sepiolite. Occurrences, Genesis and Uses. Development in Sedimentology*; Singer, A., Galan, E., Eds.; Elsevier: Amsterdam, 1984; Vol. 37, pp 253−287. (c) Galan, E. *Clay Miner.* **1996**, *31*, 443−453. (d) Murray, H. H. *Appl. Clay Sci.* **1991**, *5*, 379−395. (e) Murray, H. H. *Clay Miner.* **1999**, *34*, 39−49.

(6) (a) Weir, M. R.; Rutinduka, E.; Detellier, C.; Feng, C. Y.; Wang, Q. K.; Matsuura, T.; Le Van Mao, R. *J. Membr. Sci.* **2001**, *182*, 41−50. (b) Wang, Q. K.; Matsuura, T.; Feng, C. Y.; Weir, M. R.; Detellier, C.; Rutinduka, E.; Le Van Mao, R. *J. Membr. Sci.* **2001**, *184*, 153−163.

10.1021/cm034867i CCC: $25.00
Published on Web 12/03/2003

Scheme 1

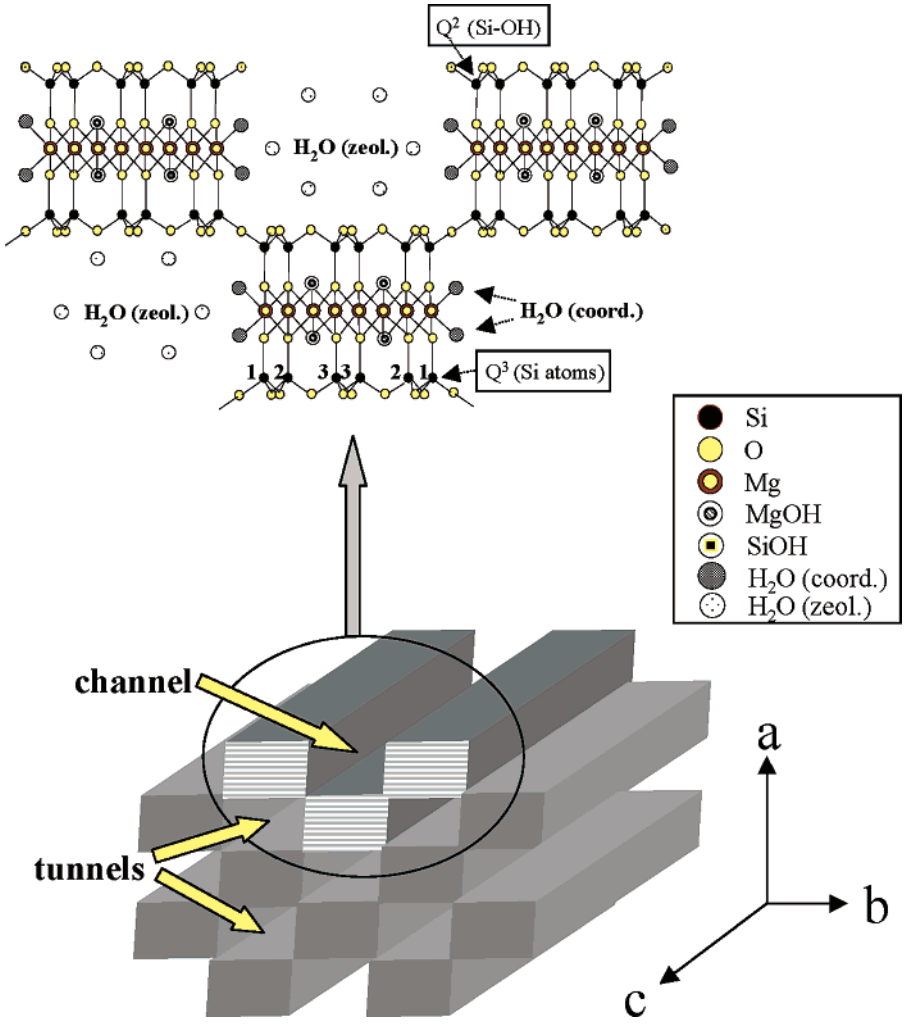

ant,[8] as a catalyst or catalyst carrier,[9] as fire-retardant painting material,[10] or as templates for the formation of carbon nanofibers[11] leads to the need to characterize its intercalation compounds. It is particularly necessary and important to comprehend the molecular processes responsible for the fixation of organic molecules in the nanostructured tunnels of sepiolite.

Sepiolite is a hydrated magnesio silicate with the theoretical half unit-cell formula $Si_{12}O_{30}Mg_8(OH,F)_4(OH_2)_4 \cdot 8H_2O$,[12] taking into account the presence of structural fluorine in sepiolite. The structure of sepiolite is derived from talc-like T−O−T ribbons that expand along the *c* direction, with a width of three pyroxene chains (Scheme 1). Each ribbon is connected to the next through an inverted Si−O−Si bond, resulting in a staggered talc layer with a continuous tetrahedral sheet and a discontinuous octahedral sheet. The discontinuous nature of the octahedral sheet allows for the formation of rectangular, tunnel-like micropores, which run parallel to the fiber axis and which are filled completely by zeolitic water $[H_2O]_{zeol}$ under ambient conditions. These nanostructured tunnels measure approximately 3.7 × 10.6 Å in cross section, and they account in large part for the high specific surface area and excellent sorptive properties of sepiolite, once the zeolitic water has been removed by thermal treatment that does not exceed 150 °C. Finally, the terminal Mg^{2+} that are located at the edges of the octahedral sheets complete their coordination with two molecules of structural water $[H_2O]_{coord}$, which are in turn hydrogen-bonded to zeolitic water molecules located within the nanopores of the magnesio silicate (Scheme 1).

Small polar molecules, such as ammonia, methanol, ethanol, or acetone, can access the tunnels of sepiolite,

(7) Le Van Mao, R.; Rutinduka, E.; Detellier, C.; Gougay, P.; Hascoet, V.; Tavakoliyan, S.; Hoa, S. V.; Matsuura, T. *J. Mater. Chem.* **1999**, *9*, 783−788.

(8) (a) Sugiura, M.; Fukumoto, S.; Inagaki, S. *Clay Sci.* **1991**, *8*, 129−145. (b) Sugiura, M. *Clay Sci.* **1993**, *9*, 33−41. (c) Casal, B.; Merino, J.; Serratosa, J. M.; Ruiz-Hitzky, E. *Appl. Clay Sci.* **2001**, *18*, 245−254. (d) Kara, M.; Yuzer, H.; Sabah, E.; Celik, M. S. *Water Res.* **2003**, *37*, 224−232.

(9) (a) Damyanova, S.; Daza, L.; Fierro, J. L. G. *J. Catal.* **1996**, *159*, 150−161. (b) Corma, A.; Martin-Aranda, R. M. *J. Catal.* **1991**, *130*, 130−137. (c) d'Espinose de la Caillerie, J.-B.; Fripiat, J. J. *Catal. Today* **1992**, *14*, 125−140. (d) Aramendía, M. A.; Borau, V.; Jiménez, C.; Marinas, J. M.; Porras, A.; Urbano, F. J.; Villar, L. *J. Mol. Catal.* **1994**, *94*, 131−147.

(10) (a) Davis, R. D.; Gilman, J. W.; Vanderhart, D. L. *Polym. Degrad. Stab.* **2003**, *79*, 111−121. (b) Devaux, E.; Rochery, M.; Bourbigot, S. *Fire Mater.* **2002**, *26*, 149−154. (c) Morgan, A. B.; Harris R. H.; Kashiwagi, T.; Chyall, L. J.; Gilman, J. W. *Fire Mater.* **2002**, *26*, 247−253. (d) Zhu, J.; Morgan, A. B.; Lamelas, F. J.; Wilkie, C. A. *Chem. Mater.* **2001**, *13*, 3774−3780.

(11) (a) Sandi, G.; Winans, R. E.; Seifert, S.; Carrado, K. A. *Chem. Mater.* **2002**, *14*, 739−742. (b) Cheng, J. P.; Tu, J. P.; Ye, Y.; Sun, Y. L.; Liu, F.; Ning, Y. S.; Kong, F. Z.; Lu, H. M.; Zhang, X. B. *Chin. Chem. Lett.* **2002**, *13*, 381−384.

(12) (a) Preisinger, A. *Clays Clay Miner.* **1959**, *6*, 61−67. (b) Santarén, J.; Sanz, J.; Ruiz-Hitzky, E. *Clay Miner.* **1990**, *38*, 63−68.

either by displacing the zeolitic water molecules or by filling the free space after the previous removal of the latter by heating or by application of dynamic vacuum.[2,3] The case of larger polar molecules is still controversial. For example, it was recently proposed that indigo molecules cover the openings of the tunnels of sepiolite after removal of zeolitic water, being also anchored in the external channels to silanol groups.[4g] They strongly reduce the tunnels access to nitrogen or argon and consequently strongly reduce the measured microporosity, but essentially leave the tunnels emptied.[4g] However, molecular dynamics simulations show that indigo molecules are free to diffuse within the tunnels of palygorskite, to reach stable sites where they are trapped.[4h] Similarly, the migration and incorporation in the tunnels of a molecule like benzene are still subject to discussions.[2c,2e,3] Given its molecular dimensions and its polarity, pyridine is a likely candidate for occupancy of the tunnels of sepiolite.[2e] The sorption of pyridine on palygorskite was shown to take place in two steps, corresponding to the formation of monolayer and bilayer coverages of the surfaces.[13] A thermal analysis of sepiolite and palygorskite treated with pyridine showed the adsorption of pyridine by both minerals, with replacement of the zeolitic and, partially, of the coordinated water molecules.[14] Selectivity in the accessibility of the tunnels was shown for pyridine and some of its derivatives.[2e,3] While pyridine can access the interior of the tunnels, 2,6-dimethylpyridine molecules are located in the external channels, not in the tunnels.[3] However, a recent study of the adsorption of 2-aminopyridine and 2,2′-bipyridyl on sepiolite indicated that these molecules not only are adsorbed on the external surfaces but also are incorporated in the channels and in the tunnels.[15]

In this paper, the incorporation of pyridine in the tunnels of sepiolite, and its modifications upon thermal treatment, are studied in detail, using various complementary characterization techniques. It is shown that the pyridine molecules are sequestered in the nanostructured porous silicate up to 450 °C, while the material is fully dehydrated. Upon incorporation in the tunnels of sepiolite at room temperature, the pyridine molecules are H-bound to the structural, Mg(II)-coordinated, water molecules. About 50% of the pyridine is lost together with the coordinated water molecules below 200 °C. This event is accompanied by coordination of the remaining pyridine molecules to the edge Mg(II) ions in the octahedral sheets, resulting in a material with a structure similar to that of the parent sepiolite, but with pyridine molecules coordinated to the Mg(II) edge cations instead of structural water molecules. This material is stable up to 450 °C. At this temperature the coordinated pyridine molecules escape from the tunnels, resulting in a collapsed sepiolite structure which can be reversibly rehydrated. The dehydroxylation of the Mg−OH groups is observed at a temperature similar to that of the parent sepiolite material, in the range 780−840 °C.

(13) Ruiz-Hitzky, E.; Casal, B.; Serratosa, J. M. *Proceedings 5th Meeting European Clay Groups*, Prague, 1985; pp 125−131.

(14) Shuali, U.; Yariv, S.; Steinberg, M.; Müller-Vonmoos, M.; Kahr, G.; Rub, A. *Clay Miner.* **1991**, *26*, 497−506.

(15) Sabah, E.; Çelik, M. S. *J. Colloid Interface Sci.* **2002**, *251*, 33−38.

Experimental Section

Materials. Two sepiolite samples from the Tajo Basin, Spain, with large similarities in their structural, textural, and composition characteristics were used in this work. The sample used for NMR and thermogravimetric studies (SepSp-1) is from Valdemoro (Madrid). It was obtained from the Source Clays Repository, of the Clay Minerals Society (Purdue University), with a chemical composition[16] (%) of SiO_2 (52.9), MgO (23.6), Al_2O_3 (2.56), Fe_2O_3 (1.22), FeO (0.3), MnO (0.13), K_2O (0.05). The crude sepiolite was purified according to previously reported procedures.[6a] The particle size was selectively restricted by passing the sepiolite samples through a 100-mesh sieve. The sample used for IR studies was from Yunclillos (Toledo). It was obtained from Tolsa S.A. Chemical analysis,[18] X-ray diffraction data, and IR spectra were used for estimation of the samples purity: sepiolite >95%. The granulometric fraction used was <200 mesh. Mineralogical analysis by X-ray diffraction[17d] showed that sepiolite contained traces of quartz and calcite. These impurities do not have a significant observable effect in the spectroscopic and thermal analysis.

Pyridine (>99.9%, HPLC grade) was obtained from Aldrich Chemical Co., or, in the case of the IR studies, was the heart-cut fraction obtained by vacuum distillation of a >99% purity reagent (Merck, spectroscopic grade), which was previously dried over an activated 4-Å molecular sieve. Pyridine-^{15}N (≥99% ^{15}N) was obtained from C/D/N Isotopes Inc.

Preparation of the Samples. Typically, sepiolite samples SepSp-1 were heated with a ramp rate of 1 °C min^{-1} to 120 °C and then kept at 120 °C for 20 h under air in a baffle furnace, to eliminate selectively the surface-bound water and zeolitic water from the nanoporous tunnels. The vials containing dried sepiolite were immediately transferred into capped bottles containing a few milliliters of pyridine (pyridine-^{15}N for the ^{15}N NMR experiments) and then remained in contact with the pyridine vapor at room temperature.

Infrared Spectroscopy. IR spectra were recorded on a Perkin-Elmer Model 580B double-beam spectrophotometer, coupled to a data station M-3500PE. Disks of 13 mm of the mineral samples, obtained by pressing (2000 kg·cm^{-2}) about 10 mg of the solid, were used as self-supported samples which were mounted in a stainless steel holder and placed in a typical IR vacuum cell with CaF_2 windows. All operations were carried out on a conventional vacuum system able to evacuate the cell to pressure in the 10^{-5} Torr range and heat the sample. On the other hand, oriented films of sepiolite were prepared by filtering aqueous clay suspensions (0.5% w/w) through a Millipore membrane.

Nuclear Magnetic Resonance Spectroscopy. Solid state ^{1}H magic-angle spinning (MAS) nuclear magnetic resonance (NMR), ^{15}N MAS and cross-polarization (CP)/MAS NMR spectra were recorded at 500.13 and 50.69 MHz, respectively, at room temperature on a Bruker Avance 500 spectrometer, using SepSp-1 samples. The typical spinning rates for ^{1}H and ^{15}N experiments were 15 and 6 kHz, respectively. The excitation pulse and recycle delay time for ^{1}H NMR were 2.0 μs and 2 s (16 scans), respectively, and the proton 90° pulse was 4.0 μs. A ramped CP pulse sequence was used for all ^{15}N NMR cross polarization experiments. The recycle delay time was 2

(16) The chemical composition data are provided as unofficial data by the Source Clays Repository (http://cms.lanl.gov/chem.htm). The chemical composition of SepSp-1 is also reported elsewhere, from the U.S. Geological Survey Spectroscopy Lab: (http://speclab.cr.usgs.gov/spectral.lib04/DESCRIPT/sepiolite.SepSp-1.html), as SiO_2 (54.8), TiO_2 (0.04), MgO (22.3), Al_2O_3 (1.39), Fe_2O_3 (0.40), FeO (0.02), MnO (<0.02), K_2O (0.20),[17a] from ref 17b as SiO_2 (63.2), TiO_2 (0.03), MgO (25.4), Al_2O_3 (1.19), Fe_2O_3 (0.22), FeO (0.08), MnO (0.01), and from ref 17c as SiO_2 (54.43), Al_2O_3 (1.5), Fe_2O_3 (0.44), MnO (0.01), MgO (22.83), CaO (0.06), K_2O (0.14), TiO_2 (0.05), P_2O_5 (0.04), Cr_2O_3 (0.0028), and NiO (0.0008).

(17) (a) Clark, R. N.; Swayze, G. A.; Gallagher, G. A.; King, T. V. V.; Calvin, W. M. *U.S. Geol. Surv., Open File Rep.* **1993**, 93−592. (b) He, C.; Makovicky, E.; Osbæck, B. *Appl. Clay Sci.* **1996**, *10*, 337−349. (c) Vogt, C.; Lauterjung, J.; Fischer, R. X. *Clays Clay Miner.* **2002**, *50*, 388−400. (d) Shuali, U.; Steinberg, M.; Yariv, S.; Müller-Vonmoos, M.; Kahr, G.; Rub, A. *Clay Miner.* **1990**, *25*, 107−119.

(18) Ruiz-Hitzky, E.; Casal, B. *J. Catal.* **1985**, *92*, 291−295.

s, and the proton 90° pulse was 4 μs. The contact time to allow the transfer of magnetization between protons and ^{15}N nuclei was 5 ms. The ^{1}H NMR signals were externally referenced to the $-CH_3$ resonance of acetone at 2.06 ppm, corresponding to tetramethylsilane (TMS) at 0 ppm. The ^{15}N NMR signals were externally referenced to the ammonium resonance of ammonium nitrate, ($^{15}NH_4$)(NO_3).

Solid state ^{29}Si MAS and CP/MAS NMR and ^{13}C MAS and CP/MAS NMR spectra were recorded at 39.75 and 50.32 MHz, respectively, at room temperature on a Bruker ASX-200 spectrometer. Typical spinning rates of 4 kHz (^{29}Si) and 5 kHz (^{13}C) were used, respectively. A ramped CP pulse sequence was used for all ^{29}Si and ^{13}C cross polarization experiments. The recycle delay time was 2 s, and the proton 90° pulse was 4 μs. The contact time to allow the transfer of magnetization between protons and ^{29}Si and ^{13}C nuclei was 10 ms for ^{29}Si and 2 ms for ^{13}C. The ^{29}Si NMR signals were externally referenced to the $-Si(CH_3)_3$ resonance of tetrakis trimethylsilylsilane at −9.9 ppm, corresponding to tetramethylsilane (TMS) at 0 ppm. The ^{13}C signals were externally referenced to the high-frequency signal of adamantane at 38.4 ppm. Quantitative ^{29}Si NMR spectra were recorded both at 99.38 and 39.75 MHz, varying the recycle delay time from 2 to 180 s, and verifying that the relative intensities of the peaks were constant.

Thermal Analysis. Differential thermal analysis (DTA), thermal gravimetric analysis (TGA), and derivative thermal gravimetric analysis (DTG) were performed on a SDT 2960 Simultaneous DSC-TGA instrument. Approximately 10−20 mg of the SepSp-1 sample was placed in a platinum crucible on the pan of a microbalance and then heated from room temperature to 1000 °C at a heating rate of 10 °C min^{-1} while being purged with gas and constantly weighed. The gases were drawn down a capillary in the SDT furnace. MS spectra were recorded on a Pfeiffer GSD 301 instrument. The mass spectrum was run in the scanning mode from mass 10 to mass 80, at a scan rate of 0.2 s per mass.

Texture Analysis. BET surface area and micropore measurements on both sepiolite samples were performed on a Micromeritics ASAP-2010 instrument (N_2 or Ar adsorption at 77 K). The samples were degassed at room temperature under vacuum on the apparatus prior to the measurement. The degas process was terminated when the vacuum pressure decreased to 3 μmHg. The molecular cross section of nitrogen used in the data analysis was 0.1620 nm^2. The typical range of thickness chosen for t-plot measurements was 3.5−5 Å.

Results and Discussion

A cross section of the structure of sepiolite along the *a* and *b* axis is shown in Scheme 1. It indicates the presence of water molecules filling the tunnels in the *c* axis direction (zeolitic water, $[H_2O]_{zeol}$), and of water molecules directly coordinated to the edge magnesium cations, to complete their coordination shell (coordinated water, $[H_2O]_{coord}$). Zeolitic water is removed by heating at around 120 °C, leaving the tunnels empty.[1b] This is apparent on the nitrogen adsorption isotherm[4g] obtained after heating sepiolite at 120 °C for 20 h or degassing at room temperature under a pressure of 3×10^{-3} Torr. The isotherm is of type I at lower relative pressures, characteristic of microporous solids.[19] An hysteresis is observed at higher relative pressures, indicative of the presence of interparticle mesopores. A t-plot analysis of the isotherm gives a micropore area of 152 m^2 g^{-1} and a volume of 77 mm^{3}g^{-1} (Table 1). The BET surface area is 298 m^2 g^{-1}, a value in good agreement with previously reported measurements on sepiolite samples from similar origin.[3,17b,20]

Table 1. BET Surface Area and Micropore Analysis from Nitrogen Adsorption Isotherms

			T-plot		Horvath−Kawazoe	
sample[a]	BET surface area (m^2 g^{-1})	C value	micropore area (m^2 g^{-1})	micropore volume (mm^3 g^{-1})	cumulative pore volume (mm^3 g^{-1})	median pore diameter (Å)
A	298	−77	152	77	137	6.3
A1	291	−76	150	75	131	6.2
A2	292	−72	158	79	138	6.4
A3	172	−279	50	25	78	7.6
A4	126	116	8	3		
B	99	91	0	0		
B2	110	101	5	1		
B3	118	80	0	0		
B4	112	104	5	1		

[a] Sample A: sepiolite (SepSp-1); samples A1−A4: sample A heated for 20 h at 120, 200, 300, and 400 °C, respectively. Sample B: sepiolite (SepSp-1) previously heated at 120 °C for 20 h and then exposed to pyridine vapor for 1 month. Samples B1−B4: sample B heated for 1 h at 120, 200, 300, and 400 °C, respectively.

The loss of zeolitic water is also apparent from thermal gravimetric analysis (TGA). A typical weight loss of 5% is observed from room temperature to 90 °C, with the first maximum observed on the differential thermogravimetric analysis (DTG) at 60 °C. The weight loss is less than 1% for the sample shown in Figure 1, which was preheated at 120 °C for 20 h. Three more weight losses are observed (Figure 1), at 260, 510, and 800−830 °C. They are attributed respectively to the loss of a first structural water, of the second structural water, and to the dehydroxylation of the internal Mg−OH.[14,20b,21] This is confirmed by mass spectrometry (MS) analysis: water gas is evolved from the material at the same temperatures (Figure 2A). The restructuration of sepiolite submitted to thermal treatment was previously discussed and interpreted.[21b,22] It has been proposed that the loss of a first structural water is accompanied by a partial collapse of the structure. This step is reversible.[2e−g,i,22] The loss of the second water molecule results in the irreversible formation of a collapsed structure. This is apparent in Table 1: when the sample is heated at 300 °C for 20 h, the micropore area drops from 150 to 50 m^{2}g^{-1}. If the sample is heated to 400 °C for 20 h, the microporosity of the material is almost completely lost: it drops to 8 m^2 g^{-1}. After dehydroxylation, enstatite is irreversibly formed, accompanied by an exothermic peak on the TGA.[21]

(19) (a) Brunauer, S. *The Adsorption of Gases and Vapors*; Princeton University Press: Princeton, NJ, 1943. (b) Webb, P. A., Orr, C. *Analytical Methods in Fine Particle Technology*; Micromeritics Instr. Corp.: Norcross, GA, 1997.

(20) (a) Grillet, Y.; Cases, J. M.; Francois, M.; Rouquerol, J.; Poirier, J. E. *Clays Clay Miner.* **1988**, *36*, 233−242. (b) Jimenez-Lopez, A.; Lopez-Gonzales, J.; Ramirez-Saenz, A.; Rodriguez-Reinoso, F.; Valenzuela-Calahorro, C.; Zurita-Herrera, L. *Clay Miner.* **1978**, *13*, 375. (c) Hibino, T.; Tsunashima, A.; Yamazaki, A.; Otsuka, R. *Clays Clay Miner.* **1995**, *43*, 391−396.

(21) (a) Ahlrichs, J. L.; Serna, C.; Serratosa, J. M. *Clays Clay Miner.* **1975**, *23*, 119−124. (b) Serna, C.; Ahlrichs, J. L.; Serratosa, J. M. *Clays Clay Miner.* **1975**, *23*, 452−457. (c) Nagata, H.; Shimoda, S.; Toshio, S. *Clays Clay Miner.* **1974**, *22*, 285−293. (d) Frost, R. L.; Ding, Z. *Thermochim. Acta* **2003**, *397*, 119−128.

(22) (a) Barron, P. F.; Frost, R. L. *Am. Miner.* **1985**, *70*, 758−766. (b) Sanz, J. Distribution of ions in phyllosilicates by NMR spectroscopy. In *Absorption Spectroscopy in Mineralogy*; Moltana A., Burragato, F., Eds.; Elsevier Sci. Publ.: Amsterdam, 1990; pp 103−144. (c) Weir, M. R.; Kuang, W.; Facey, G. A.; Detellier, C. *Clays Clay Miner.* **2002**, *50*, 240−247.

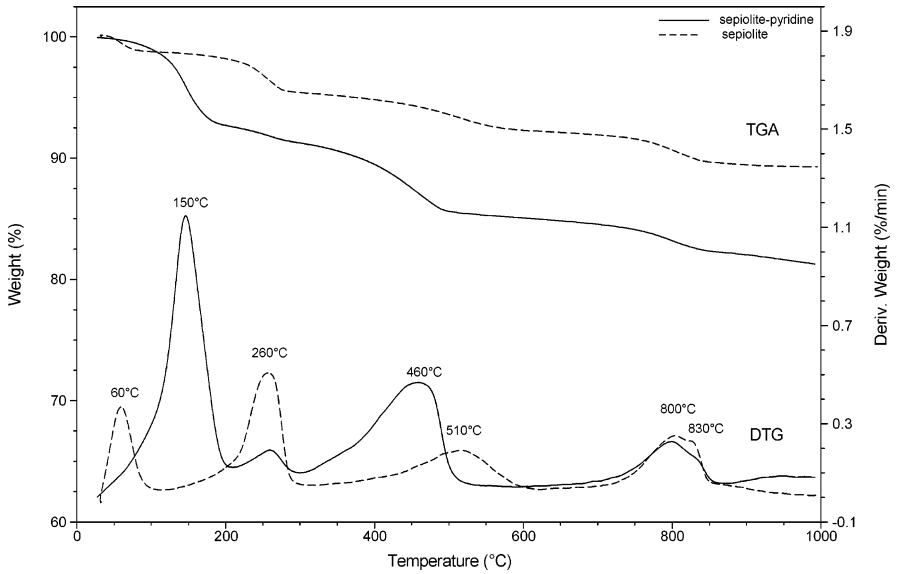

Figure 1. TGA and DTG of sepiolite (SepSp-1) previously heated at 120 °C for 20 h (- - -) and of the same sample exposed to pyridine for a month (—).

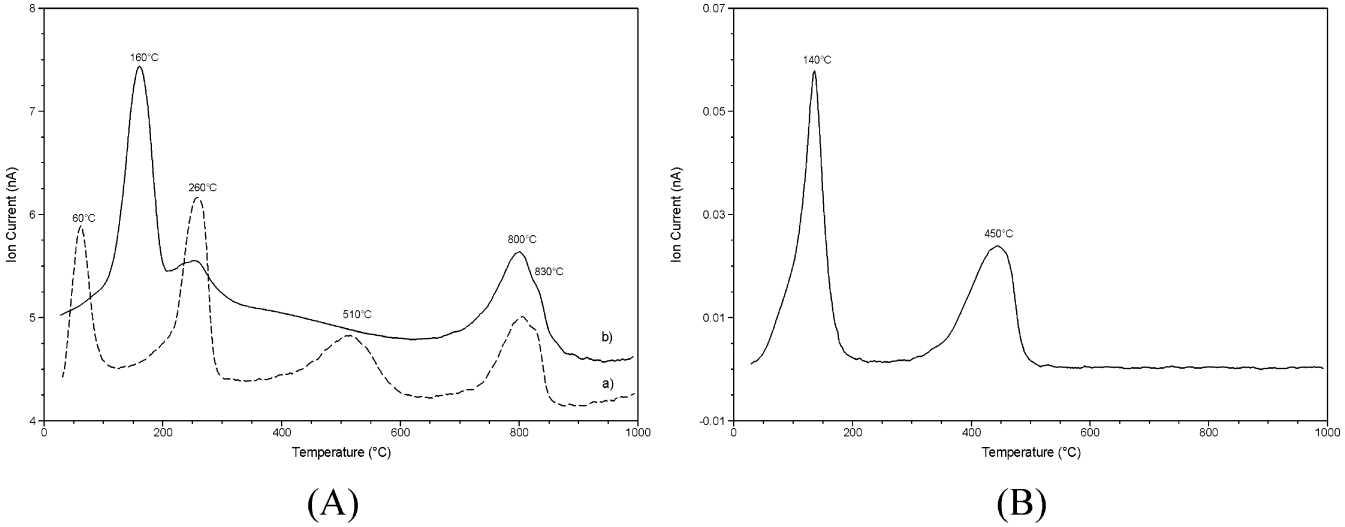

Figure 2. Mass spectrometry of water ($m/e = 18$) (A) for (a) sepiolite (SepSp-1), (b) sepiolite previously heated at 120 °C for 20 h and then exposed to pyridine for a month, and of pyridine ($m/e = 79$) (B) for sample (b).

An Horvath−Kawazoe analysis[23] of the adsorption isotherm gives a median pore diameter of 6.3 ± 0.1 Å for the samples heated to 200 °C for 20 h, keeping the microporosity of the original sepiolite sample. This value is in agreement with previously reported values[3] and is in good agreement with the idealized crystallographic structure of sepiolite and the dimension of its tunnels. Further heating at 300 °C produces a collapse of the structure as evidenced by the loss of microporosity and a modification of the median pore diameter for the remaining micropores.

The measured micropore volume of 77 $mm^3\ g^{-1}$ is due to the tunnels extending in the *c* direction. Since the cross section of the tunnels is 3.7 × 10.6 Å, the tunnels have a total length of approximately 2×10^{11} m for each gram of sepiolite. For comparison, the distance from the sun to the earth is 1.496×10^{11} m. Obviously, the estimated length of the tunnels corresponds to the sum of individual sections, which are much shorter. From a SEM picture,[6a] one can estimate approximately at 5−10 μm the typical length of a sepiolite individual fiber. This is more than 10 000 times the typical dimension of a relatively small molecule, such as pyridine (6.65 × 3.34 × 6.48 Å).[24] Consequently, one can expect that the process of filling the tunnels by molecular diffusion is slow, particularly in the case of a polar, coordinating molecule such as pyridine. Typically, to ensure a full incorporation, a sepiolite sample from which the zeolitic water molecules have been removed is put in contact with pyridine vapor for a month. It is our experience that the same result could be achieved after 3 days (see Figure 3).

The material resulting from the incorporation of pyridine in sepiolite has completely lost its microporosity (Table 1). While zeolitic water is removed from hydrated sepiolite by degassing at room temperature

(23) Horvath, G.; Kawazoe, K. *J. Chem. Eng. Jpn.* **1983**, *16*, 470−475.

(24) Webster, C. E.; Drago, R. S.; Zerner, M. C. *J. Am. Chem. Soc.* **1998**, *120*, 5509−5516.

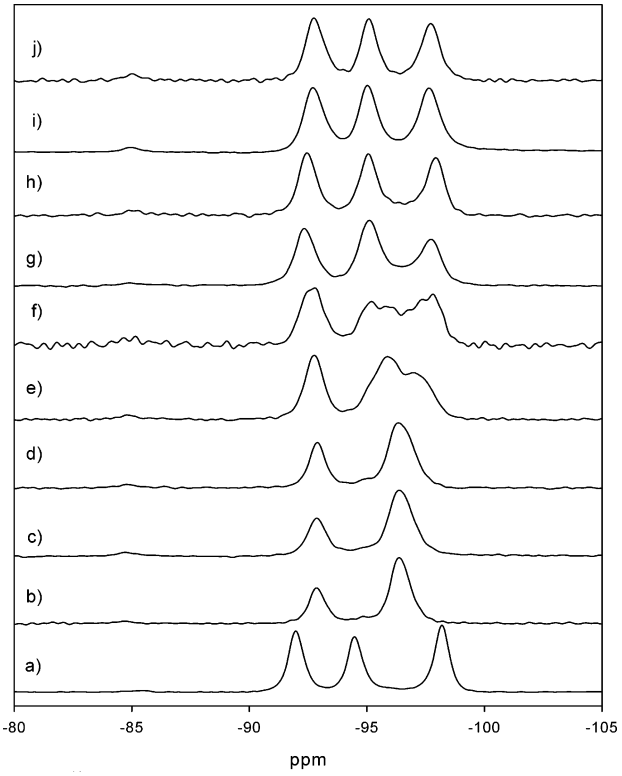

Figure 3. ^{29}Si CP/MAS NMR spectra (39.75 MHz) of (a) sepiolite (SepSp-1); (b) sepiolite heated at 120 °C for 20 h; (c−j) sepiolite previously heated at 120 °C for 20 h and then exposed to pyridine-d_5 for 1 min (c), 3 min (d), 7 min (e), 8.5 min (f), 10 min (g), 15 min (h), 27 h (i), and 9 days (j).

(Table 1, sample A), pyridine molecules are not removed by the same treatment (Table 1, sample B). This will be further confirmed below by independent IR and NMR studies on two sepiolite samples. The BET surface area drops from 298 to 99 m^2g^{-1}, corresponding to the complete loss of microporosity which drops from 152 to 0 m^2g^{-1}. Interestingly, the textural properties of pyridine−sepiolite are almost insensitive to thermal treatment of the material, up to heating at 400 °C for 1 h (Table 1, samples B1−B4).

Figure 1 shows the thermal gravimetric analysis of the pyridine−sepiolite adduct, under a flux of He, obtained after submitting the zeolite-dehydrated sepiolite sample to the presence of pyridine vapor for 1 month. Major changes can be observed on the TGA and the DTG traces. Four weight losses are observed, at 150, 260, 460, and 800−830 °C. The nature of the gases evolved is given by mass spectrometry analysis. Figure 2A indicates loss of water at 160, 260, and 800−830 °C. Figure 2B indicates loss of pyridine at 140 and 450 °C. Similar results were obtained for TGA and DTG when the nature of the flux gas was changed from He to N_2 or air. In the case of the DTA analysis, an exothermic peak was observed at 400 °C in air only, which can be attributed to the combustion of the remaining pyridine molecules, before their desorption.[14]

From the textural and thermal analysis results, one can draw the following conclusions.

(i) The zeolitic water molecules filling the tunnels of sepiolite (SEP) are removed by heating at 120 °C or by degassing under dynamic vacuum (3×10^{-3} Torr) at room temperature. The resulting zeolite-dehydrated sepiolite, keeping structural water molecules coordinated to the edge Mg(II) cations (SEP−SW), is characterized by micropore area and volume of 152 $m^2\ g^{-1}$ and 77 $mm^3\ g^{-1}$, respectively.

(ii) When submitted to pyridine vapors for several days, SEP−SW incorporates pyridine molecules in its tunnels. Since the structural water molecules are still present, one can hypothesize that the incorporated pyridine molecules are linked to the sepiolite structure through H-bonds to the structural water molecules. In other words, pyridine occupies the second coordination shell of Mg(II). This pyridine−sepiolite material (SEP−SW−PYR) has no measurable microporosity.

(iii) Most of the structural water of SEP−SW−PYR is lost at 140 °C, together with approximately 50% of the pyridine. Only a small fraction (±5%) of the structural water is lost at the same temperature as for the original sepiolite sample, at 250 °C. At this stage, the only guest in the tunnels is pyridine. It is hypothesized that the pyridine molecules are coordinated directly to Mg(II). In other words, pyridine replaces water in the first coordination shell of Mg(II). As the previous one, this pyridine−sepiolite material (SEP−PYR) has no measurable microporosity.

(iv) The coordinated pyridine molecules are removed from SEP−PYR upon further heating of the sample at 450 °C. The dehydroxylation of the MgOH groups can be observed in the same range of temperatures as the original sepiolite sample, around 800 °C. An exothermic peak on the DTA indicates the formation of enstatite at 830 °C.

Consequently, from the textural and thermal analysis, two well-defined, different adducts of pyridine with sepiolite can be evidenced, SEP−SW−PYR and SEP−PYR. The infrared and multinuclear NMR spectroscopic studies reported below will further characterize these two materials and test the hypothesis presented above.

At this point, a short discussion on the morphology of the sepiolite particles and the potential adsorption sites of pyridine is helpful. Scheme 2 gives an idealized representation of the cross section of sepiolite fibers. Typical dimensions of 250 × 40 Å were reported for the Vallecas sepiolite,[1b] corresponding approximately to nine unit cells in width and only three in thickness, since the units cells cross section are 26.95 × 13.37 Å.[1b] More generally, widths range between 100 and 300 Å and thicknesses between 50 and 100Å.[1a] The model of Scheme 2 is 230 × 60 Å, in the expected dimension range. This morphology translates in several types of adsorption sites for guest molecules. In addition to the tunnels (T in Scheme 2), there are external channels of two types, depending upon the dimension of their opening, 10.6 or 3.7 Å (respectively C1 and C2 in Scheme 2). The two adsorption sites, C1 and C2, are very different. While the adsorbed molecules interact with one silica surface only on C1 sites, they interact with two silica surfaces on C2 sites, in a manner similar to the adsorption in tunnels, on the T sites. In that respect, C2 and T sites should behave similarly and display similar microporosity characteristics. In addition, there are sites on external surfaces (E1 and E2 in Scheme 2). It is to be noted that a coordinating molecule such as pyridine can bind to Mg(II) sites (through

Scheme 2

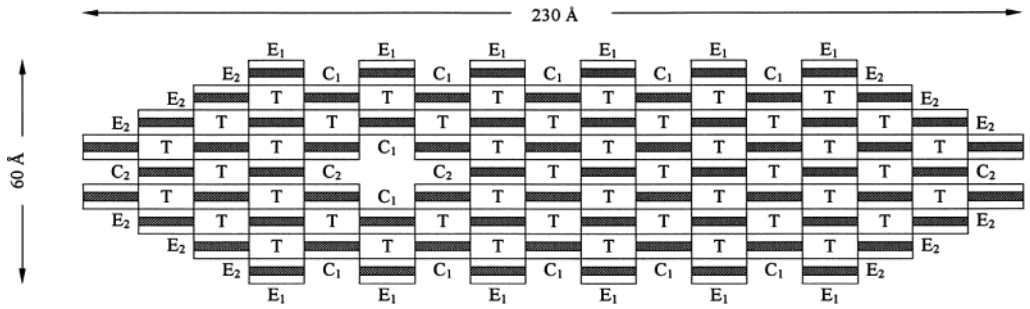

coordinated water, or not) in T, C1, C2, and E2 sites. It can also be hydrogen-bonded to external silanol Q^2 groups bordering the external surfaces, including those of the channels.

The model of Scheme 2 is obviously idealized and oversimplified, but the possibility of larger tunnels, resulting from possible irregular succession of the sepiolite unit cells, is indicated. It gives an illustration of the heterogeneity of the potential adsorption sites, characterized by microporous (T and C2 sites) and external (E and C1 sites) surface area. Taking into consideration the fact that only one of the two silicate surfaces of the tunnels and of the C2 channels is measured from the nitrogen adsorption isotherm, the number of silicate surfaces of each type, available for nitrogen adsorption, is similar (the model of Scheme 2 gives a ratio of 1 to 1.4 for external (E and C1) surfaces over microporous (C2 and T) surfaces). This is in good agreement with the BET measurements, giving a micropore surface area of 152 $m^2\ g^{-1}$ and an external surface area of 146 $m^2\ g^{-1}$. This represents about 50% of external/internal structural blocks ratio, which is in good agreement with the ratio deduced from high-resolution TEM images and IR spectroscopy ($\gamma_{SiOH}/\gamma_{MgOH}$),[25] as well as from the ratio of Q^2(Si−OH) over Q^3 quantitative ^{29}Si MAS NMR signals. The quantitative ^{29}Si MAS NMR spectrum of sepiolite is given in Figure 4. The assignments of the ^{29}Si NMR signals were reported previously.[22] The low-frequency signal was attributed to the edge Si (noted 1 in Scheme 1), which, according to the structural model of sepiolite, is replaced by Q^2(SiOH) at the borders of external surfaces. Accordingly, the sum of the integrations of the edge and of the Q^2 signals (8.0) is equal to the integrations for the near edge (2) and center (3) signals (average: 8.1), in excellent agreement with the structural model and with the signals assignments.[22] The experimental quantitative ratio of Q^2 over Q^3 is 1:23. This is in reasonable agreement with the morphology model of Scheme 2, giving an idealized ratio of 1:17.

The molecular volume of pyridine[24] is 144 Å^3, considering pyridine as a rectangular box of dimensions 6.65 × 3.34 × 6.48 Å. This volume is more appropriate than the molar volume corresponding to molecular packing since in the confined environment of the tunnels a non-negligible amount of space remains empty. The micropore volume was measured to be 77 $mm^3\ g^{-1}$ (Table 1). This value is in excellent agreement with the isotherm

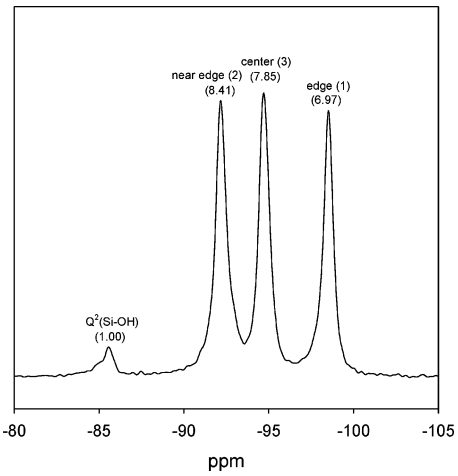

Figure 4. ^{29}Si quantitative MAS NMR spectra (99.38 MHz) of sepiolite. The integrations are indicated. The numbering corresponds to Scheme 1.

of adsorption on sepiolite of pyridine in hexane, giving an adsorption amount of 1.8×10^{-3} mol g^{-1}. Considering, on the basis of the nitrogen adsorption data, that approximately 50% of the pyridine is adsorbed in the tunnels, one can calculate a micropore volume of 78 $mm^3\ g^{-1}$. Moreover, from the same data, one can calculate that the mass % of pyridine in the micropores of sepiolite is 7.0%. Consequently, the model is also in good agreement with thermal analysis data since this value corresponds to the mass % observed on the TGA in the weight loss step in the range 300−500 °C (6.0%, T + C2 sites). A shoulder should be noted around 380−400 °C, corresponding tentatively to C2 sites. The weight loss observed at 150 °C corresponds to a weight loss of 5.6% of pyridine (8.6% to be corrected for the concomitant loss of water estimated at 3% from the value obtained on the parent sepiolite sample), to be compared with the 6% loss in the range 300−453 °C. Again, one can observe an approximately equal distribution of the two families of adsorption sites.

The morphological considerations above are in good agreement with the proposed model. SEP−SW−PYR loses externally adsorbed pyridine (C1 and E2 sites) at 140 °C. It is remarkable that this loss is accompanied by a complete restructuration of the sepiolite structure since, in a synergistic manner, most of the structural, Mg(II) coordinated water is lost, while pyridine replaces water in the first coordination sphere of Mg(II), despite the known remarkable ability of water to stabilize Mg(II).[26] One can suggest that the driving force for the process is the extra stability that pyridine brings to the system by additional van der Waals interactions with

(25) Ruiz-Hitzky, E. Contribution à l'étude des réactions de greffage de groupements organiques sur les surfaces minérales. Greffage de la sépiolite. Thèse de doctorat, Université Catholique de Louvain, 1974.

the silicate surfaces in the tunnels. Moreover, if the diffusional escape of water molecules from the tunnels is relatively unhindered, this is not the case for the larger, polarizable, aromatic pyridine molecule. One can envision the pyridine molecules as being "trapped" in the tunnels, coordinating the Mg(II) coordination sites made vacant by the release of water. Remarkably also, and in complete agreement with this scenario, once cooled and allowed in air in the presence of water vapor, sepiolite reverts back to its original structure. In summary, SEP−PYR is a thermodynamically unstable structure, kinetically formed at high temperatures, giving extra stability to the sepiolite channels nanostructures (up to 400 °C the structure of sepiolite does not collapse when pyridine is trapped).

The following infrared and multinuclear NMR spectroscopic studies characterize further the pyridine−sepiolite materials, supporting the model presented above. Vibrational spectroscopy studies of sepiolite were recently reported.[28] The IR spectra in the 4000−2600-cm^{-1} region[3] show the extinction of the band at 3720 cm^{-1}, assigned to the OH stretching vibrations of the sepiolite silanol groups,[21a] whereas the band at 3680 cm^{-1} assigned to the ν_{OH} of hydroxyl groups linked to the octahedral Mg^{2+} ions remains unaltered.[3] The shift of the 3720-cm^{-1} band involving the hydrogen bonding with the surface silanol groups is a reversible process because the ν_{OH} band of the Si−OH groups is completely restored after heating under vacuum treatment (250 °C, 3 h). The band at 3680 cm^{-1} (ν_{OH} of MgOH groups) inside the structural blocks remains unaltered after pyridine adsorption, in agreement with the inaccessibility to these hydroxyl groups. A marked change is observed in the broad band assigned to the ν_{OH} vibrations characteristic of the H_2O molecules present in the mineral (3630 and 3550 cm^{-1}: coordinated water; 3385 and 3276 cm^{-1}: zeolitic water).[3] Their shift to lower frequencies results from hydrogen-bonding interactions with adsorbed pyridine.

On the other hand, in the 1800−1300 cm^{-1} region the IR spectra show the bands characteristic of the ν_{CC} vibrations of pyridine absorbed and the $\delta_{(HOH)}$ of the water molecules on the mineral substrate, respectively. So bands at 1626 and 1617 cm^{-1}, assigned to the coordinated water in starting sepiolite,[29] are perturbed, showing a decrease in their relative intensity (Figure 5) and a shift toward higher frequencies attributed to the hydrogen bonding with the pyridine molecule. As these bands are assigned to coordinated water associated to Mg(II) at the edges of structural blocks mainly located in the internal structural cavities (*tunnels*) of the solid, their perturbation indicates the penetration of pyridine inside such cavities. In this same spectral region (1800−1300 cm^{-1}) four bands assigned to the ν_{CC} vibrations of pyridine are also observed (Table 2). Their position and relative intensity are compared with pure pyridine and pyridine adsorbed on various solids of different nature.[27] Therefore, the moderate surface acidity of sepiolite can be exclusively ascribed to Lewis sites. Brönsted centers are not detected as the 1540-cm^{-1} band characteristic of the pyridinium ions are not observed in the sepiolite−pyridine IR spectra.

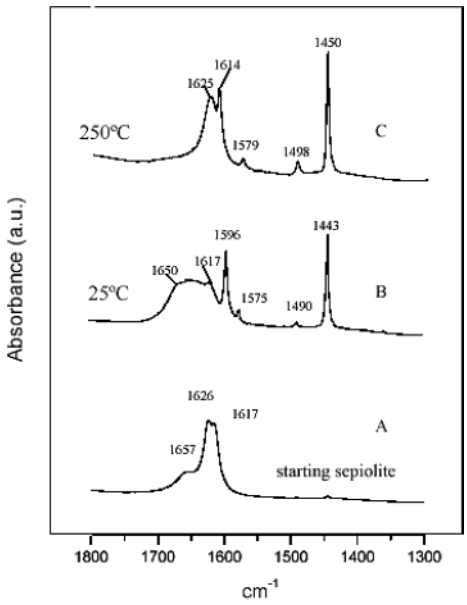

Figure 5. IR spectra (1800−1300 cm^{-1} region) of natural sepiolite (A) and sepiolite exposed to pyridine vapors. (B) Sample degassed at 25 °C. (C) Sample degassed at 250 °C.

The role of coordinated water as adsorption sites of pyridine acting as "water bridges" can also be deduced by analysis of the IR spectrum registered in this 1800−1300-cm^{-1} region (Figure 5). Changes in these bending vibrations bands (at about 1620 cm^{-1}) are observed after thermal treatment under dynamic vacuum (250 °C, 3 h). According to Serna et al.,[29] under these conditions, the coordinated water molecules of sepiolite are partially removed. This is also observed when pyridine molecules are present, and it is accompanied by the shift of the 1596- and 1443-cm^{-1} absorption bands of adsorbed pyridine to 1614 and 1450 cm^{-1}, respectively. These last bands can be assigned to the direct coordination of the pyridine molecule to the Mg(II) located at the edges of the structural blocks. This is a reversible process, as indicated by the recovery of the initial IR spectra after rehydration. Scheme 3 illustrates the proposed mechanism that resumes the ascribed interactions between pyridine and the different adsorption sites on the sepiolite surface.

Figure 3 gives the ^{29}Si CP/MAS NMR spectra of sepiolite (Figure 3a). Three peaks characteristic of the three different crystallographic positions of Si atoms in sepiolite (see Scheme 1) can be observed at −92.0, −94.5, and −98.3 ppm. They have been attributed[22] respectively to near edge (2), center (3), and edge (1) Si atoms. Upon heating at 120 °C for 20 h, the two peaks

(26) Walker, N.; Dobson, M. P.; Wright, R. R.; Barran, P. E.; Murrell, J. N.; Stace, A. J. *J. Am. Chem. Soc.* **2000**, *122*, 11138−11145.

(27) (a) Parry, E. P. *J. Catal.* **1963**, *2*, 371−379. (b) Basila, M. R.; Kantner, T. R.; Rhee, K. H. *J. Phys. Chem.* **1967**, *68*, 3197−3207. (c) Farmer, V. C.; Mortland, M. M. *J. Chem. Soc. (A)* **1966**, 344−351. (d) Ward, J. W. *J. Catal.* **1969**, *14*, 365−378. (e) Letaïef, S.; Casal, B.; Aranda, P.; Martín-Luengo, M. A.; Ruiz-Hitzky, E. *Appl. Clay Sci.* **2003**, *22*, 263−277. (f) Falabella Sousa-Aguiar, E.; Doria Camorim, V. L.; Zanon Zotin, F. M.; Correa dos Santos, R. L. *Microporous Mesoporous Mater.* **1998**, *25*, 25−34. (g) Avram, M.; Mateescu, Gh. D. *Spectroscopie Infrarouge. Applications en Chimie Organique*; Dunod Ed.: Paris, 1970.

(28) (a) McKeown, D. A.; Post, J. E.; Etz, E. S. *Clays Clay Miner.* **2002**, *50*, 667−680. (b) Frost, R. L.; Cash, G. A.; Kloprogge, J. T. *Vib. Spectrosc.* **1998**, *16*, 173−184. (c) Frost, R. L.; Locos. O. B.; Ruan, H.; Kloprogge, J. T. *Vib. Spectrosc.* **2001**, *27*, 1−13.

(29) Serna, C.; Rautureau, M.; Prost, R.; Tchoubar, C.; Serratosa, J. M. *Bull. Groupe Fr. Argiles* **1975**, *26*, 153−163.

Table 2. Frequency and Assignment of IR Absorption Bands (1400−1700 cm^{-1} Region) of Pyridine Adsorbed on Sepiolite, Compared with the Bands Observed in the Spectra of Pure Pyridine and Pyridine Adsorbed on Other Porous Solids[a]

pyridine adsorbed on other solids						
sepiolite (degassed at 25 °C)	sepiolite (degassed at 250 °C)	hydrogen bonding (Pyr..H)	Lewis centers (Pyr:L)	Brönsted centers ($PyrH^+$)	pure pyridine (liquid)[1]	assignment
1443 (vs)	1450 (vs)	1440−1447[b] (vs) 1445[c] 1446[e] 1445[f] (vs), 1440[f] (sh)	1447−1460[b] (vs) 1450[d] 1452[g]	1540[b] (s) 1550[c] 1545[e] 1545[h] (m) 1543[i] (m)	1439	$B_1$19b
1490 (w)	1498 (w)	1485−1490[b] (w) 1491[c] 1494[f] (w)	1488−1503[b] 1490[d] 1496[g] (m)	1485−1500[b] 1491[h] (s) 1489[i] (s)	1482	$A_1$19a
1577 (w)	1579 (w)	1580−1600[b] 1575[c] 1584[f] (w)	1580[b] (v) 1579[g] (w)	1620[b] (s) 1620[h] (s) 1619[i] (s)	1572	$B_1$8b
1596 (s)	1614 (s)	1614[b] 1597[c] 1602[f] (s)	1600−1633[b] (s) 1604[d] (s), 1580[d] (s) 1615[g] (s)	1640[b] (s) 1638[h] (s) 1631[i] (s)	1583	$A_1$8a

[a] Intensities: w = weak; m = medium; s = strong; vs = very strong; v = variable; sh = shoulder. [b] Silica−alumina, cracking catalysts.[27a,b] [c] Mg−montmorillonite.[27c] [d] Anhydrous Cu−montmorillonite.[27c] [e] Mg−zeolite X.[27d] [f] Palygorskite degassed at 25 °C (Casal and Ruiz-Hitzky, unpublished results). [g] Palygorskite degassed at 300 °C (Casal and Ruiz-Hitzky, unpublished results). [h] Al/Fe−montmorillonite PILC.[27e] [i] La−zeolite NaY.[27f]

Scheme 3

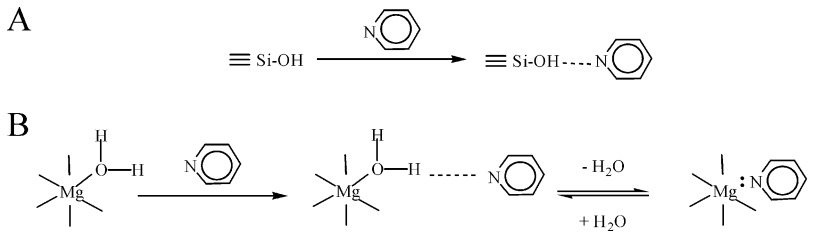

at −94.5 and −98.3 ppm collapse in a higher intensity signal at −96.5 ppm, while the third signal slightly shifts from −92.0 to −93.0 ppm. This ^{29}Si NMR spectrum is characteristic of zeolite-dehydrated sepiolite (SEP−SW).[2g] Figure 3c−j gives the ^{29}Si CP/MAS NMR spectra of SEP−SW exposed to pyridine vapors for various amounts of time. The same experiment was performed under MAS conditions with similar results. When the equivalent experiment was done in the case of acetone, a recovery of the initial three peaks of the ^{29}Si NMR spectrum could be observed when acetone was incorporated in the tunnels of sepiolite[2g] in less than a minute at room temperature. The results are comparable in the case of pyridine. Gradually over time, the characteristic ^{29}Si NMR spectrum of sepiolite is recovered. After 15 min the recovery is almost complete. After 9 days, three well-resolved signals at −92.7, −95.1, and −97.7 ppm are obtained. 2-D COSY and HETCOR experiments demonstrate an attribution of the peaks identical to that of the original sepiolite sample, respectively near edge (2), center (3), and edge (1) (see Scheme 1).[22]

The presence of a ^{29}Si NMR signal of low intensity, at −85.0 ppm, previously attributed to Q^2(Si−OH), is also observed. This experiment indicates that the original structure of sepiolite is recovered after exposure of SEP−SW to pyridine vapors, in agreement with the formation of SEP−SW−PYR. The ^{29}Si NMR results are in agreement with the incorporation of PYR in the tunnels.

Further evidence comes from the ^{13}C NMR spectra. Figure 6a gives the ^{13}C MAS NMR spectra of SEP−SW−PYR obtained after exposure of SEP−SW to pyridine for 1 month. The MAS NMR spectrum gives signals at 149.2, 135.4, and 123.3 ppm for the ortho, para, and meta carbons, respectively. These chemical shift values are almost identical to the chemical shifts observed for

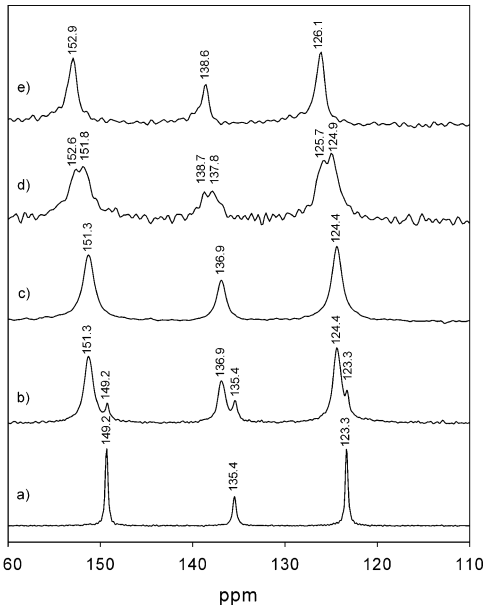

Figure 6. ^{13}C NMR spectra (50.32 MHz) of sepiolite (SepSp-1) previously heated at 120 °C for 20 h and then exposed to pyridine for a month: (a) MAS; (b) CP/MAS; (c) CP/MAS on sample (a, b) heated at 90 °C for 10 h; (d) CP/MAS on sample (a, b) heated to 300 °C with a ramp of 10 °C min^{-1}; (e) CP/MAS on sample (d) kept at 300 °C for 1 h.

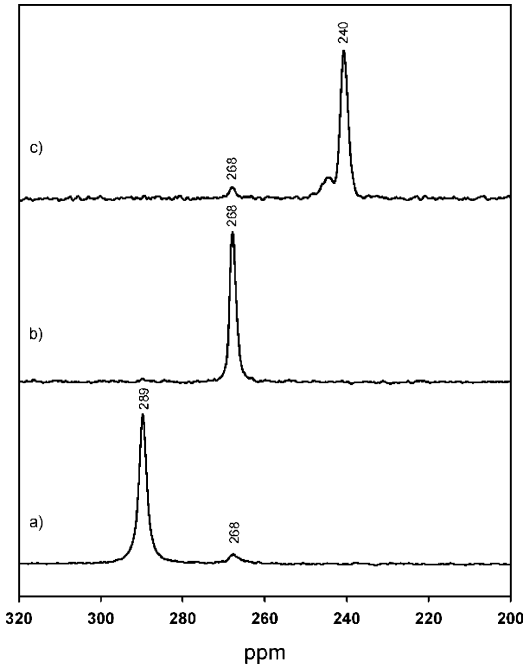

Figure 7. ^{15}N NMR spectra (50.69 MHz) of sepiolite (SepSp-1) previously heated at 120 °C for 20 h and then exposed to pyridine-^{15}N for 10 days: (a) MAS; (b) CP/MAS; (c) CP/MAS on sample (a, b) heated at 300 °C for 0.5 h.

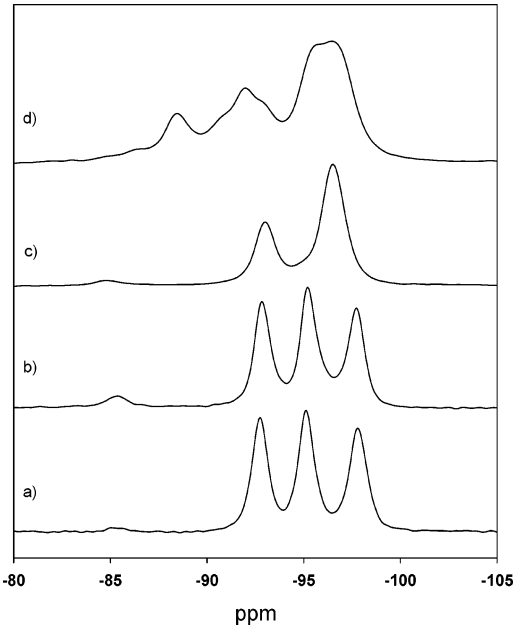

Figure 8. ^{29}Si CP/MAS NMR spectra (39.75 MHz) of sepiolite (SepSp-1) previously heated at 120 °C for 20 h and then exposed to pyridine for a month, and then heated to 200 °C (a) and 300 °C (b), in comparison with sepiolite heated for 20 h at 200 °C (c) and at 300 °C (d).

the pure solvent, not corrected for magnetic susceptibility (respectively 150.3, 136.0, and 124.0 ppm). The CP/MAS spectrum on the same sample shows in superposition to these signals three other peaks, more intense and broader, at 151.3, 136.9, and 124.4 ppm. Their line width is in the range 58−70 Hz, compared to line width in the range 18−24 Hz for the MAS spectrum. Gentle heating of the sample at 90 °C for 10 h leads to the removal of the first series of peaks, the narrower ones. These results can be interpreted as evidence for the fixation of two different types of PYR on sepiolite: mobile PYR molecules, on the external surfaces and in the C1 channels, and PYR molecules more rigidly fixed inside the tunnels and the C2 channels. The former ones are detected by the MAS NMR experiment, while the latter ones, detected only by CP/MAS, give broader signals due to chemical shift dispersion effects resulting from imperfect local order. After further heating to 300 °C, the CP/MAS spectrum shows a major change, with the replacement of the three signals of Figure 6c by three different signals, further shifted to higher frequency. Three types of pyridine molecules are clearly identified on the ^{13}C NMR spectra: (i) externally, loosely, bound pyridine molecules in multilayers, (ii) pyridine molecules occupying the channels and tunnels of the SEP−SW−PYR material, and (iii) pyridine molecules in the SEP−PYR material, coordinated to Mg(II).

A similar experiment was done using ^{15}N MAS and CP/MAS NMR. Pyridine-^{15}N (≥99% ^{15}N) was incorporated in sepiolite using a procedure similar to the one used for the ^{13}C NMR experiment. The results are given in Figure 7. The MAS spectrum gives a major signal at 289 ppm and a minor signal at 268 ppm. The ^{15}N static NMR gives one signal centered at 289 ppm. The signal at 289 ppm can be attributed to externally, loosely bound pyridine molecules in multilayers. Its chemical shift is close to the one of bulk liquid pyridine. The CP/MAS NMR spectrum on the same sample gives only one signal, at the same position as the minor one on the MAS spectrum, 268 ppm. It can be attributed to pyridine molecules adsorbed in the tunnels of SEP−SW−PYR. Heating the sample at 300 °C for 0.5 h results in a major change: the signal at 268 ppm has almost disappeared and is replaced by a new signal at 240 ppm. This new signal, still observed when the sample is heated at 400 °C for 0.5 h, can be attributed to the pyridine molecules in SEP−PYR, directly coordinated to the Mg(II) edge cations. These results confirm the ^{13}C NMR and the IR results and support the hypothesis of the incorporation of PYR in two steps: first, H-bonding of PYR to structural water molecules and then direct coordination of PYR to edge Mg(II), replacing water in the first coordination shell of Mg(II).

The following series of experiments demonstrate that the structure of sepiolite is stabilized by the direct coordination of PYR to edge Mg(II) cations. It has been previously shown that heating sepiolite above 300 °C results in a collapse of the structure. This is particularly apparent on the ^{29}Si NMR spectra, where more than three signals can be observed, corresponding to a partial collapse of the structure after removal of the first structural water molecule.[22] Figure 8 gives the ^{29}Si CP/MAS NMR spectra of SEP−SW−PYR. As described above, it is characterized by three Q^3 signals at −92.8, −95.2, and −97.7 ppm and a minor Q^2 signal at −85.0 ppm. Quite remarkably, in strong contrast with the sepiolite sample, heating the sample to 200 °C and even to 300 °C does not notably modify the spectrum. This is in agreement with a model in which the pyridine molecules remain in the tunnels, bound to Mg(II), at temperatures up to 300 °C (see also Figures 1 and 2B), preserving the general structure of sepiolite and particularly the integrity of the tunnels structure. It must be noted also that the Q^2 (SiOH) signal is insensitive to the thermal treatment.

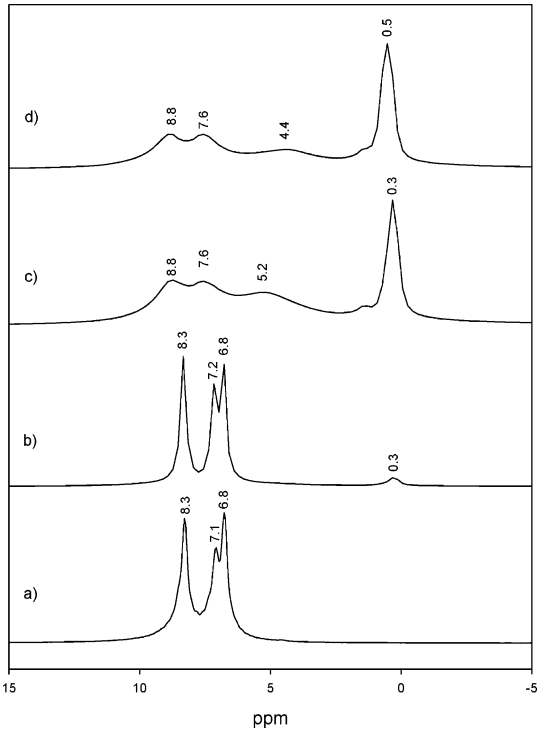

Figure 9. (a) ^{1}H NMR spectum (500.13 MHz) of pure liquid pyridine; (b) ^{1}H MAS (15 kHz) NMR spectrum of sepiolite (SepSp-1) previously heated at 120 °C for 20 h and then exposed to pyridine for a month; (c) and (d): ^{1}H MAS (15 kHz) spectra of sample (b) heated for 0.5 h at 200 and 300 °C, respectively.

Further information on the structure of SEP−PYR can be obtained from dichroism and ^{1}H NMR measurements. The band at 750 cm^{-1} assigned to out-of-plane vibrations of symmetry class B2 of pyridine adsorbed on sepiolite shows a dichroic character as it increases in intensity by changing the incidence angle of the IR beam from 0 to 45°. This behavior, together with the non-dichroic effect observed in the bands close to 1450, 1490, 1580, and 1600 cm^{-1}, indicates that the pyridine ring lies parallel to the plane defined by the sepiolite film, that is, the (*b*,*c*) plane, as it was reported in pyridine and pyridinium species intercalated in layer silicates.[30] The IR results showing that the adsorbed molecules are oriented parallel to the [100] plane of the sepiolite are in agreement with ^{1}H NMR data. The ^{1}H MAS NMR spectra of SEP−SW−PYR and SEP−PYR were recorded at 500 MHz with a relatively high spinning rate of 15 kHz, to remove most of the dipolar couplings.[31] Similarly to what was observed in ^{13}C and ^{15}N NMR experiments, liquid-type pyridine is observed on the ^{1}H spectrum of the sample submitted to pyridine vapors (Figure 9b). Heating the sample removes these mobile, externally adsorbed pyridine molecules, resulting in a dramatic change of the ^{1}H spectrum (Figure 9c,d). While the *o*- and *m*-pyridine ^{1}H NMR signals are slightly shifted to lower fields, as it is expected from coordination of pyridine to Mg(II), a major upfield shift is observed for the para ^{1}H NMR signal: it shifts to 5.2 ppm when the sample is heated at 200 °C for 0.5 h and to 4.4 ppm when the sample is heated at 300 °C for 0.5 h. This upfield shift can be attributed to diamagnetic anisotropies resulting from the spatial positioning of the pyridine molecules in the tunnels. TGA and adsorption isotherms (see above) give a stoichiometry of 1 PYR for 2 terminal Mg(II), corresponding to the structure $Si_{12}O_{30}Mg_8(OH,F)_4$(PYR). This is in agreement with a filling of the tunnels by coordinated pyridine molecules in an alternate arrangement parallel to the (*b*,*c*) plane since terminal Mg(II)'s are separated by 5.2 Å along the *c* axis and by 16 Å along the *b* axis. The silicate surfaces are separated by 3.7 Å (*a* axis) and, consequently, are ideally positioned to strongly interact by van der Waals interactions with the π electronic densities of the coordinated pyridine molecules. This results in stability to the system, providing the driving forces for the formation of an otherwise unstable structure. Quite logically then, upon exposure to water at room temperature, the system reverts back to its original structure (Scheme 3).

This textural, thermal, and spectroscopic study of the materials resulting from the incorporation of pyridine molecules in sepiolite demonstrates that a truly remarkable nanohybrid material is formed through the direct coordination of pyridine to the Mg(II) coordination sites of the nanostructured tunnels of sepiolite. This structure is formed kinetically at high temperatures when the sepiolite tunnels are dehydrated and the pyridine molecules are trapped in the tunnels. The close fit of the π electronic density of pyridine with the silicate surfaces separated by 3.7Å, coupled with the direct coordination of pyridine to edge Mg(II) sites, provides the driving force for the formation of this highly structured alternating alignment of pyridine molecules in the confined environment of the nanostructured tunnels. The unambiguous elucidation of this structure by complementary experimental techniques leads to the design of new, highly structured, nanohybrid materials based on remarkable, naturally occurring magnesio silicates.

In addition, one should note that the sequestration of molecules in the micropores of fibrous silicates may explain the high stability of the "Maya Blue" pigment.[4] Indigo molecules can be trapped in the entrance of the tunnels or in the channels, specially in those of type C2 (Scheme 2).[4g]

Finally, this investigation puts clearly in evidence the particular features of sepiolite. This silicate, together with palygorskite, are usually classified as members of the clay minerals family constituting the so-called *hormite group*. However, many of its structural characteristics—and consequently its textural behaviors—are closely related to zeolites. Sepiolite could be in fact regarded as a "magnesium-based zeolite" showing tunnels of equal dimensions filled with water molecules that can be replaced by other molecular species such as pyridine. Intrinsic charge of sepiolite is very low (few exchangeable cations) and molecules do not protonate but are retained when sorbed into the tunnels or channels by other mechanisms, resulting in the sequestration within the structural cavities. Thus, sepiolite can be considered as an intermediate member between clay minerals (smectites) and zeolites or as a zeotype mainly composed by silicon and magnesium with properties close to the clay phyllosilicates family.

(30) Serratosa, J. M. *Clays Clay Miner.* **1966**, *14*, 385−391.
(31) Brown, S. P.; Spiess, H. W. *Chem. Rev.* **2001**, *101*, 4125−4155.

Acknowledgment. The Natural Sciences and Engineering Research Council of Canada (NSERC; discovery grant program) and the CICYT, Spain (projects: MAT2000-0096-P4-02, MAT2000-1585-C03-01, and MAT2000-1451) are gratefully thanked for financial support. The "Secretaria de Estado de Educación y Universidades" of Spain is gratefully acknowledged for financial support of the stay of C.D. in the CSIC (Madrid) during a sabbatical leave.

CM034867I